effect on the performance of the motor if it were not expected. Thus, it is apparent that under some circumstances the effects of spin rate on motor performance can be significant.

The effect of motor spin rate on thrust and total impulse will be determined by the nozzle configuration. In the case of a convergent-divergent nozzle, the angular velocity of the combustion gases theoretically will decrease in the diverging section. If the diameter of the nozzle exit is equal to the chamber diameter, the exit velocity of the gases will be unaffected by the spin rate. In this case the instantaneous thrust would be increased because of the increased flow rate (for $n > 0$), but the total impulse would be unchanged.

Even though this analysis is highly idealized, it indicates the nature and approximate magnitude of the effect caused by spinning a solid-propellant motor with an end-burning grain. A similar analysis could be conducted for a motor with an internal-burning grain. In this case, the flow field would be more complex and time-dependent. For a simple, internal-burning cylindrical grain, all streamlines would emerge with equal angular momentum, and the field would be irrotational, or true vortex flow. An analysis of this condition has been carried out by Mager[2] who has shown that a reduction in effective throat area occurs as was found in the present case. A further complication to the problem would be the use of propellants whose combustion products contain condensed phases. If this case should warrant investigation, it might best be approached experimentally.

The implication of this analysis is that solid-propellant motors, which are intended to operate at high rates of spin, should be tested while spinning. Otherwise, actual performance characteristics may be significantly different from those observed during test firings.

References

[1] Allan, D. S., Bastress, E. K., and Knapton, D. A., "Design studies on a 105 mm gun boosted rocket," Final Report, Arthur D. Little, Inc., Contract No. DA-19-020-ORD-5695 (January 25, 1963); classified.

[2] Mager, A., "Approximate solution of isentropic swirling flow through a nozzle," ARS J. **31**, 1140–1148 (1961).

Spike Penetration Dynamics

GEORGE S. CAMPBELL*
University of Connecticut, Storrs, Conn.

THE use of nose spikes is a familiar technique for terminal recovery of missiles. Such a technique has a potential use for landing payloads on the moon or planets. It therefore seems appropriate to develop methods that will minimize the amount of empirical information used in the design of such a landing system. An extensive study of landing dynamics was reported in Ref. 1, a numerical technique was presented for estimating spike penetration, and a specific example was solved. In the present note, an analytical method is presented for making preliminary estimates of penetration and loads resulting from spike impact at speeds that are low compared with the sound speed in the solid material. Its accuracy remains to be checked by appropriate tests.

Analysis

The initial motion of a spike-landing device is calculated for application to landing-loads estimation. Initial motion is defined as the time between first ground contact and reversal of the spike tip's lateral motion. The spike approaches the ground with a vertical velocity component U_0 and a horizontal component V_0. The problem is simplified by assuming a truncated wedge shape for the spike (Fig. 1). Use of a more complicated, axially symmetric geometry does not appear warranted until the soil model assumed is subjected to experimental verification. The center of gravity of the body is located at x_c, y_c, and the tip of the spike is located at x_t, y_t. During the initial period of motion, the spike moves laterally in the positive Y direction simultaneously with its vertical penetration. The lateral velocity of the tip is approximately

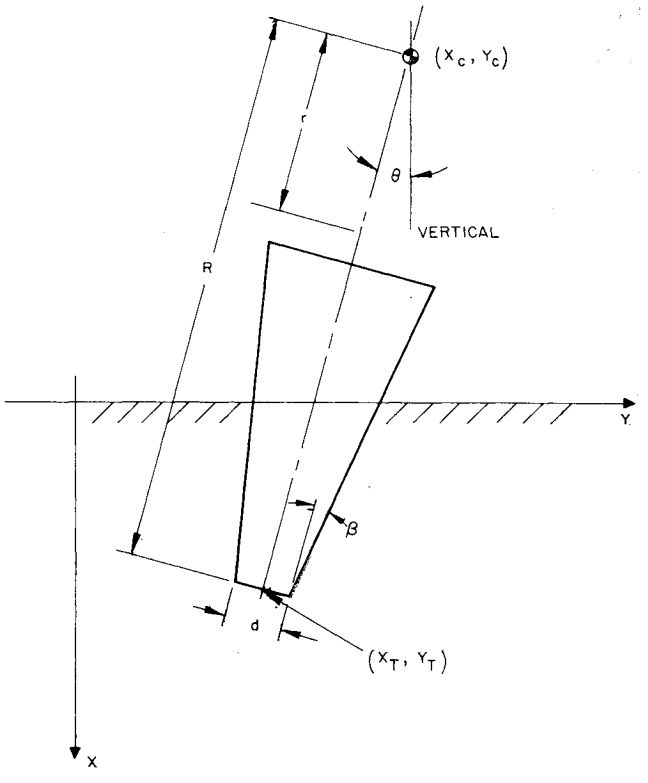

Fig. 1 Spike geometry.

$$v = V - R(d\theta/dt) \tag{1}$$

provided that $\theta \ll 1$. The end of the initial period is defined as the time at which v becomes zero. The vertical motion of the spike during the initial period is calculated from the relation†

$$\left.\begin{aligned}(d^2x_t/dt^2) + kx_t &= -K\\ k &= (\sigma L/m)(\tan\beta + \mu)\\ K &= \sigma Ld/m\end{aligned}\right\} \tag{2}$$

A bearing stress σ is assumed to act on the flat base and on the side that is moving in the Y direction. A frictional stress $\mu\sigma$ acts on one side of the spike. Consideration of forces on one side only is appropriate for slender spikes for which $\beta < \tan^{-1}(V_0/U_0)$. After the initial motion considered in this note, both sides of the wedge become effective in resisting penetration.

The bearing resistance σ depends on the shear strength of the soil.[2] Instantaneous soil strength may, in certain cases, be many times larger than values measured under static loading and should be used for estimating spike loads and trajectories. If the initial velocity is comparable to sound speed in the medium, resisting forces are expected to

Received August 31, 1964. The author wishes to express his appreciation to the Hughes Aircraft Company for their support of this work, which was performed on a consulting arrangement.

* Professor and Head of Aerospace Engineering Department. Associate Fellow Member AIAA.

† This is an approximate equation of motion, which neglects the difference between d^2x_c/dt^2 and d^2x_t/dt^2.

be velocity-dependent. Velocity dependence also exists for loosely compacted soils for which compaction waves are significant.[3]

The solution of Eq. (2) is

$$x_t = (K/k)(\cos\tau - 1) + (U_0/k^{1/2})\sin\tau \quad (3)$$

in which $\tau = k^{1/2}t$. For small values of τ,

$$x_t = U_0 t - (K/2)t^2 + \ldots \quad (4)$$

Lateral motion of the center of gravity is calculated from

$$m(d^2y_c/dt^2) = -\sigma L\, x_t \quad (5)$$

The angles β and θ are assumed small in calculating the side force on the spike $\sigma L\, x_t$. This equation, as well as Eq. (2), is applicable only during the initial motion for which $v \geq 0$ at all of the points along the spike. For the general forcing function x_t [given by Eq. (3)], the solution of Eq. (5) is

$$\eta = \cos\tau + (k^{1/2}U_0/K)\sin\tau + (\tau^2/2) + (k^{1/2}U_0/K)[(kmV_0/\sigma LU_0) - 1]\tau - 1$$

where

$$\eta = (k^2m/K\sigma L)y_c$$

The lateral velocity is

$$V = (K\sigma L/k^{3/2}m)(d\eta/d\tau)$$

For small values of τ,

$$V = V_0 - (\sigma LU_0/2m)t^2 + \ldots \quad (6)$$

The final equation defining the initial spike motion is the moment equation

$$I(d^2\theta/dt^2) = R\sigma L x_t \quad (7)$$

This equation assumes that $x_t \ll R$. The forcing function x_t is given by Eq. (3); for zero initial conditions the solution of Eq. (7) is

$$(d\theta/dt) = (\sigma LR/Ik)[(K/k^{1/2})(\sin\tau - \tau) + U_0(1 - \cos\tau)]$$

or, for small τ, is

$$(d\theta/dt) = (\sigma LRU_0/2I)t^2 + \ldots \quad (8)$$

Equations (6) and (8) are substituted into Eq. (1) in order to determine the time duration of the initial motion (i.e., when $v = 0$). Thus

$$t_c^2 = [2mIV_0/\sigma LU_0(R^2m + I)] \quad (9)$$

This equation is correct to second order in τ. The penetration depth x_t at time t_c is given by Eq. (4). For cases in which τ_c is not a small quantity compared with unity, the complete expressions for V and $d\theta/dt$ may be used in Eq. (1) to obtain t_c. The primary result of this analysis is given in Eq. (9). The value of x_t corresponding to t_c determines the side loading on the spike σLx_t and the inertia loads along the missile, given by

$$(dF/dr) = [(dm/dr)](\sigma Lx_t)[(1/m) + (rR/I)]$$

In order to approximate an axially symmetrical spike, an effective wedge width L may be chosen by equating the projected side area of a cone frustum to the side area of the wedge, so that

$$L = d_F + x_t \tan\beta_F$$

in which d_F and β_F are, respectively, tip diameter and semi-apex angle of the frustum. In this case, the initial penetration x_t is obtained from the approximate relation

$$x_t^2(d_F + x_t \tan\beta_F) = [2mIU_0V_0/\sigma(R^2m + I)]$$

The foregoing procedure is useful for calculating the shape of the lower portion of a spike so that lateral acceleration limits on the missile are not exceeded. The upper portion of the spike would then be shaped so as to maximize the area under the force-penetration curve for given spike length and maximum longitudinal deceleration. The longitudinal calculation is relatively simple, even for an axially symmetric spike, because just one degree of freedom is involved rather than three as in the calculation of lateral motion.

References

[1] Ferguson, T. R., Mollick, J., and Kitts, W. W., "A rational method for predicting alighting gear dynamic loads," Air Force Flight Dynamics Lab., Rept. ASD-TDR-62-555, Vols. I and II (December 1963).

[2] Jumikis, A. R., *Soil Mechanics* (D. Van Nostrand Co., Princeton, N. J., 1962), Chap. 22.

[3] Serbin, H., "Propagation of intense shock waves into the earth," J. Acoust. Soc. Am. **32**, 1257–1262 (1960).

An Ablation-Type Plasma Generator

GERHARD FRIND*

General Electric Company, Philadelphia, Pa.

ELECTRIC arcs can produce stable plasma streams for minutes, or even hours.[1, 2] However, they are, in general, restricted to the heating of gases; fluids and solids can be injected into the plasma streams emerging from these heaters, but this procedure decreases the flow enthalpy. They also appear to be limited with respect to attainable enthalpy of the plasmajet,[3] primarily because the steady-state heat-transfer capability of the copper walls of the arc chamber is $\leq$ 10 kw/cm^2,[4] and a substantial fraction of the electrical input is always lost to the walls. In another type of arcing device, the arc is contained in a vortex of liquid[5]; the arc evaporates the liquid and heats the vapors up to plasma temperature. Although extremely high temperatures have been reached, this type of arc heater has found no widespread application.

In this note, a plasma generator is described which uses solid ablating walls for the arcing chamber. An advantage is that the plasmajet can be discharged from a chamber at a location different from the electrode region; this keeps the contamination level low, even at extremely high power in-

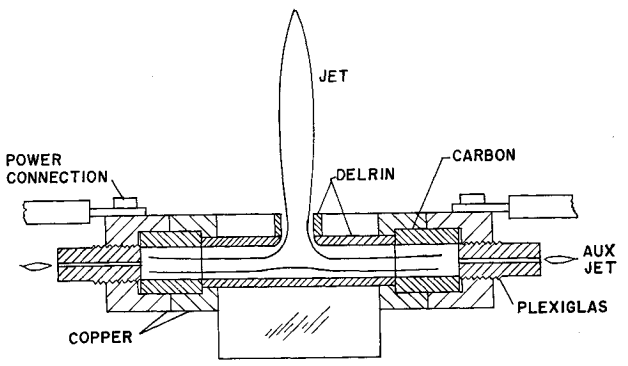

Fig. 1 Principal arrangement of ablation-type plasma generator.

Received July 20, 1964; revision received November 23, 1964. The work reported herein is part of the Research Program on Arc Plasma of the Aeronautical Research Laboratories, Office of Aerospace Research of the U. S. Air Force, whose support is acknowledged. The author wishes to thank J. J. Narbus for his assistance in design and development and for numerous good suggestions.

* Senior Project Scientist.